Journal of Organometallic Chemistry 695 (2010) 2030–2038

Contents lists available at ScienceDirect

Journal of Organometallic Chemistry

journal homepage: www.elsevier.com/locate/jorganchem

DFT study of the mechanism of Cu(I)-catalyzed and uncatalyzed intramolecular cyclopropanation of iodonium ylides

Christos E. Kefalidis [a], Argyrios A. Kanakis [b], John K. Gallos [b], Constantinos A. Tsipis [c,*]

[a] Institut Charles Gerhardt, Universite Montpellier 2, CNRS 5253, case courrier 1501, Place Eugene Bataillon, 34095 Montpellier, France
[b] Laboratory of Organic Chemistry, Department of Chemistry, Aristotle University of Thessaloniki, Thessaloniki 541 24, Greece
[c] Laboratory of Applied Quantum Chemistry, Department of Chemistry, Aristotle University of Thessaloniki, Thessaloniki 541 24, Greece

ARTICLE INFO

Article history:
Received 4 April 2010
Received in revised form
8 May 2010
Accepted 10 May 2010
Available online 15 May 2010

Keywords:
Cyclopropanation
Iodonium ylides
Mechanism of cyclopropanation
DFT calculations
Cu-catalyzed cyclopropanation

ABSTRACT

The mechanism of the Cu(I)-catalyzed and uncatalyzed intramolecular cyclopropanation of ketoesteric and diesteric iodonium ylides has been thoroughly explored by means of electronic structure calculation methods (DFT). All crucial reaction steps encapsulated in the entire catalyzed and uncatalyzed reaction pathways were scrutinized, while the elementary steps, the intermediates and transition states were identified through monitoring the geometric and energetic reaction profiles. It was found that CuCl efficiently catalyze the cyclopropanation of iodonium ylides only for their diesteric derivatives and their diazo analogues via stabilization of the respective carbene upon complexation with the metal center. For the ketoesteric iodonium ylides the CuCl catalyst does not affect the kinetics of the intramolecular cyclopropanation reactions which could proceed easily without the catalyst, in line with available experimental observations.

1. Introduction

Bicyclo[3.1.0]hexane derivatives of the general formulas **1** and **2** and related systems shown in Scheme 1 are attractive and often sought synthetic targets, because of the specific versatility and the ubiquitous occurrence of the cyclopentane ring in natural and non-natural products and biologically active compounds. These systems have been extensively used in the synthesis of steroids, prostanoids, vitamin D analogues, terpenoids, amino acids and carbocyclic nucleosides [1–16]. The best developed and most general method used so far for the construction of **1** and **2** is the catalytic intramolecular cyclopropanation of iodonium ylides **3** and **4**, or diazocarbonyl compounds **5** and **6**, both yielding essentially the same products [17,18]. However, the former have been introduced as the non-toxic substitutes of the hazardous diazo compounds.

Among the myriad of stoichiometric and catalytic processes known for the construction of cyclopropane rings, those using transition-metal catalysts have received growing attention in recent years [1–15]. In particular, chiral Cu(I)-catalyzed intramolecular cyclopropanation of unsaturated diazocarbonyl compounds yielded high enantioselectivities. The mechanism of the transition metal-catalyzed carbene transfer from diazo compounds to carbon–carbon double bonds, *via* a metal carbenoid intermediate has been extensively investigated [1–15,19]. In contrast, the transition metal-initiated iodonium ylide decomposition towards cyclopropanation products is much less established and is still controversial from a mechanistic point of view [20,21].

The majority of the synthetically important reactions with phenyliodonium ylides catalyzed by Cu(I) compounds has not been established so far. The mechanism by which cyclopropanation reactions proceed with phenyliodonium ylides using Cu(I) catalysts remains a subject of debate. Müller and co-workers [22–25] have proposed that treatment of active cyclopropanation catalysts with phenyliodonium ylides or diazo compounds, both form the same metal carbene intermediate (Scheme 2). To the contrary, Moriarty and co-workers [26–29] have placed greater value on the subtle differences in reactivities observed between phenyliodonium ylides and diazo compounds and have proposed alternative mechanistic pathways. Irrespective of the mechanism, however, the reactivities between the phenyliodonium ylides and diazo compounds are indeed quite similar in cyclopropanation reactions [22–25].

Moriarty and co-workers [26–29] in the first seminal discovery of novel CuCl-catalyzed intramolecular cyclopropanations of iodonium ylides proposed a stepwise mechanism involving electrophilic addition of the iodonium center to the double bond followed by reductive elimination of iodobenzene to afford the cyclopropane ring (Scheme 3).

* Corresponding author. Tel.: +30 2310622087.
E-mail address: tsipis@chem.auth.gr (C.A. Tsipis).

0022-328X/$ – see front matter © 2010 Elsevier B.V. All rights reserved.
doi:10.1016/j.jorganchem.2010.05.013

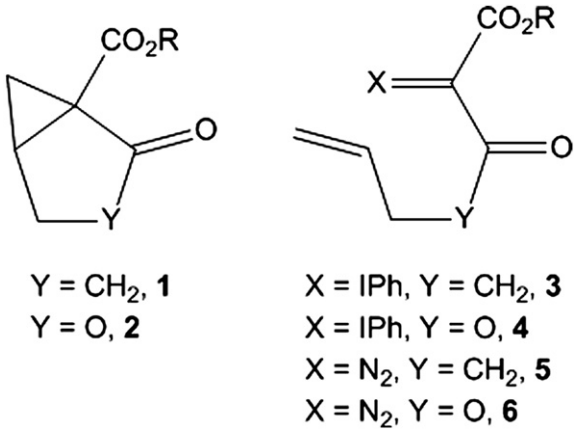

Scheme 1.

According to the mechanism proposed by Moriarty et al. [26–29], the cyclopropanation reaction does not take place in the coordination sphere of the metal, and, therefore, no asymmetric induction is to be expected if the decomposition of the iodonium ylide is effected by a chiral catalyst. Actually, the resulting diastereoselectivities from the cyclopropanation reaction were almost completely reversed between phenyliodonium ylides and the corresponding diazo compounds [20,21]. However, the role of transition-metal catalysis in these reactions remains obscure.

Recently, Müller et al. [22–25] observed a substantial degree of asymmetric induction in Cu(I)-catalyzed intramolecular cyclopropanations of some iodonium ylides, which is consistent with a carbenoid mechanism. However, a competing uncatalyzed and unselective secondary reaction may intervene at room temperature. Phenyliodonium ylides have shown both theoretically and experimentally to be good sources of free carbenes under thermal, photochemical, and catalytic conditions [30].

To gain a deeper insight into the mechanism of the transition metal-catalyzed intramolecular cyclopropanation of iodonium ylides, and understand their intricacies and catalytic events a comprehensive and consistent picture of the catalytic cycle has been derived by means of electronic structure calculations methods at the DFT level of theory. All crucial reaction steps encapsulated in the entire catalyzed and uncatalyzed courses have been scrutinized, while the elementary steps, the intermediates and transition states have been identified through monitoring the geometric and energetic reaction profiles.

2. Computational details

In view of the good performance of density functional theory (DFT), we were instigated to perform DFT calculations at the B3LYP level of theory on all stationary points of the potential energy surfaces (PES) we studied using the GAUSSIAN03 program suite [31]. The equilibrium and transition structures were fully optimized

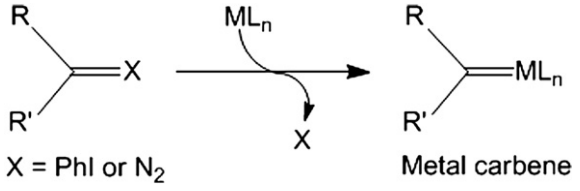

Scheme 2. The formation of the same metal carbene intermediates in the metal-catalyzed cyclopropanation of iodonium ylides and diazo compounds.

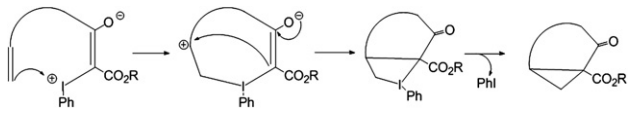

Scheme 3. Proposed reaction mechanism for the intramolecular cyclopropanation of phenyliodonium ylides.

at the Becke's 3-Parameter hybrid functional [32,33] combined with the Lee–Yang–Parr [34] correlation functional developed as B3LYP method by Stephens et al. [35,36] using the DGDZVP basis set for the I atom and the 6–31G(d) basis set for the rest of the non metal atoms. We will denote the computational approach used as B3LYP/6–31G(d)∪dgdzvp(I). B3LYP method works well in transition-metal chemistry [37] providing good descriptions of reaction profiles, including geometries, heats of reactions, and barrier heights [37–39], while it has been shown to yield good bond energies for copper compounds [40]. In all computations no constraints were imposed on the geometry. For transition states geometry determination, quasi-Newton transit-guided (QSTN) computations were performed [41]. Moreover, corrections of the transition states have been confirmed by Intrinsic Reaction Coordinate (IRC) calculations, while Intrinsic Reaction Paths (IRPs) [42] were traced from the various transition structures to make sure that no further intermediates exist. Furthermore, solvation effects were introduced using single-point PCM calculations on gas-phase optimized geometries at the B3LYP/6–31G(d)∪dgdzvp(I) level. All reported energies of the species correspond to the sum of the gas-phase free energy corrections along with PCM energies [43–45]. Dichloromethane was used as solvent for all calculations. Unless otherwise stated, only reaction energies $\Delta_R G^{solv}$ are used for the discussion on the relative stabilities of the chemical structures considered.

3. Results and discussion

For this task, the reaction trajectory of the following copper(I)-catalyzed and uncatalyzed intramolecular cyclopropanations of phenyliodonium ylides was explored (Scheme 4).

3.1. Uncatalyzed radical cyclopropanation mechanism

The calculated geometric and energetic reaction profiles for the uncatalyzed intramolecular cyclopropanation of ketoesteric, **3** and diesteric, **4** iodonium ylides are depicted schematically in Fig. 1.

The first reaction step involves the dissociation of phenyliodide molecule from the α,α'-dioxomethylene iodonium ylides **3** and **4** to form "free" ketoesteric, **7** and diesteric, **8** carbene (or carbenoid) molecules, via transition states $\mathbf{TS_{3-7}}$ and $\mathbf{TS_{4-8}}$ with activation barriers estimated at 15.5 and 20.3 kcal/mol, respectively. It has been well established both theoretically and experimentally that phenyliodonium ylides are good sources of "free" carbenes under thermal, photochemical, and catalytic conditions [30]. Therefore, it

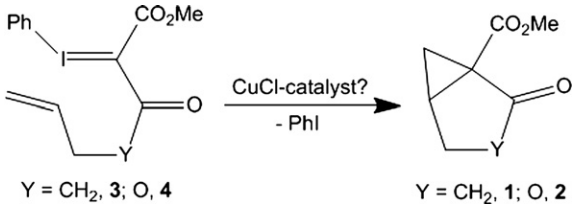

Scheme 4. Cu(I)-catalyzed intramolecular cyclopropanation of ketoesteric and diesteric phenyliodonium ylides.

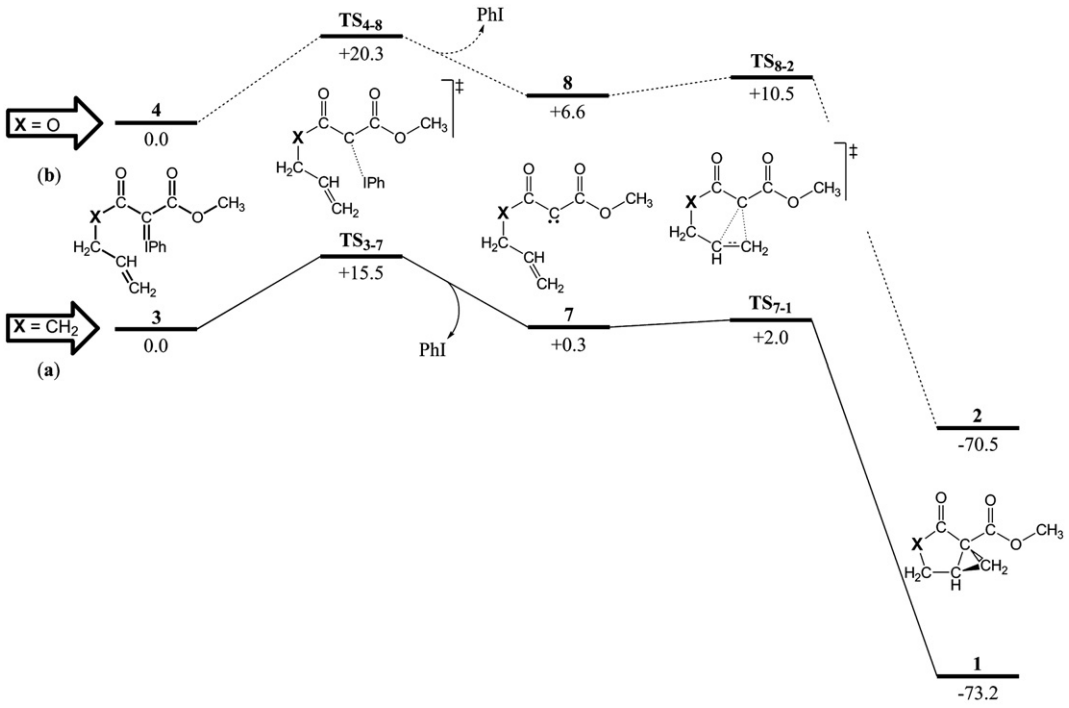

Fig. 1. Energetic ($\Delta_R G^{solv}$, in kcal/mol) and geometric reaction profiles for the uncatalyzed intramolecular cyclopropanation of ketoesteric (a) and diesteric (b) phenyliodonium ylides computed at the B3LYP/6–31G(d)∪dgdzvp(I) level of theory.

is expected phenyliodonium ylides in solutions to be in thermodynamic equilibrium with their dissociation products namely iodobenzene and "free" carbenes. In this context we thought it would be advisable to compare the dissociation processes of phenyliodonium ylides **3** and **4** and the respective diazo compounds **5** and **6**, using electronic structure calculation techniques. It was found, that the ketoesteric phenyliodonium ylides can be easily dissociated to form "free" ketoesteric carbene, **7** with dissociation energy of 13.6 kcal/mol, while for the diesteric carbene, **8**, the dissociation energy was found to be 17.7 kcal/mol. Actually, the thermal dissociation of the iodonium ylides yielding carbenes is a facile process, requiring an enthalpy change of no more than 15 kcal/mol [30]. The diesteric carbene **8** adopts the triplet as the ground state with the singlet state found to be only 0.5 kcal/mol higher in energy at the B3LYP/6–31G(d) level of theory. On the other hand, the triplet state of the ketoesteric carbene **7** was found 1.5 kcal/mol higher in energy than the singlet ground state. Furthermore, the dissociation of the respective diazo compounds **5** and **6** to dinitrogen and "free" ketoesteric, **7** and diesteric, **8** carbene molecules demands much higher energies amounted to 35.1 and 37.9 kcal/mol, respectively, verifying the experimental observations that no reaction happens in diazo compounds in the absence of a catalyst.

The equilibrium geometries of the diazo compounds **5**, **6**, the transition states $\mathbf{TS_{5-7}}$ and $\mathbf{TS_{6-8}}$, the ketoesteric, **7** and diesteric, **8** carbene molecules computed at the B3LYP/6–31G(d)∪dgdzvp(I) level of theory are shown in Fig. 2. Selected electronic parameters of the diazo compounds **5** and **6**, the phenyliodonium ylides **3** and **4**, the ketoesteric, **7** and diesteric, **8**, carbene molecules have been collected in Table 1.

It can be seen that the C–$C_{carbene}$ bond lengths of the carbene moieties in the diazo compounds are longer than the respective C–$C_{carbene}$ bond lengths of the corresponding phenyliodonium ylides (Fig. 2), while the C–$C_{carbene}$–C bond angle is almost equal in **3** and **5**, and slightly smaller in the phenyliodonium ylide **4** than in the diazo compound **6**. This observation accounts well for the computed lower X–$C_{carbene}$ bond dissociation energies of phenyliodonium ylides than the diazo counterparts due to the smaller deformation needed by the resulting "free" carbenes to adopt their ground state configuration.

According to the Natural Bond Orbital (NBO) population analysis (Table 1) the central iodine atom acquires positive natural atomic charge of 0.91 and 0.94 |e| in phenyliodonium ylides **3** and **4**, respectively, thus becoming electrophilic center. The electrophilicity index was found to be 1.78 and 1.68 for **3** and **4**, while the natural electron configuration is $5s^{1.77}5p^{4.28}$ and $5s^{1.77}5p^{4.26}$, respectively (Table 1). In contrast, the nitrogen atom directly bonded with the carbene carbon atom acquires negligible positive natural atomic charge of 0.09 and 0.11 |e| in **5** and **6**, respectively. The computed hardness η values illustrate that the diesteric derivatives are slightly more stable than the ketoesteric ones (Table 1) with respect to their dissociation. The higher values of the interaction energies of the diazo compounds are consistent with the inefficient intramolecular cyclopropanation of the diazo compounds observed experimentally, which proceeds only in the presence of CuCl catalyst [1–15]. It is also evident that cyclopropanation of the diesteric phenyliodonium ylides would proceed much slower and the use of a catalyst would be mandatory, compared to the ketoesteric phenyliodonium ylides which are consistent with experimental observations [20,21]. The extrusion of phenyliodide step (Fig. 1) in the case of the ketoesteric phenyliodonium ylide corresponds to a thermoneutral process, while the diesteric one is endergonic, in strong support of the aforementioned observations. Finally, the rate-limiting step in both paths was found to be the dissociation step.

To account for the instability of the iodonium ylides with respect to dissociation the :C–IPh bonding mode has been analyzed. The computed Mayer bond orders of 1.49 indicate that the C–IPh bond acquires a partial double bond character. It should be noticed that the C–IPh bond length is much shorter than the Ph–I bond (2.099 vs 2.181 Å for **3**; and 2.081 vs 2.179 Å for **4**). Moreover, the computed bond overlap population (*bop*) illustrates that the C–IPh

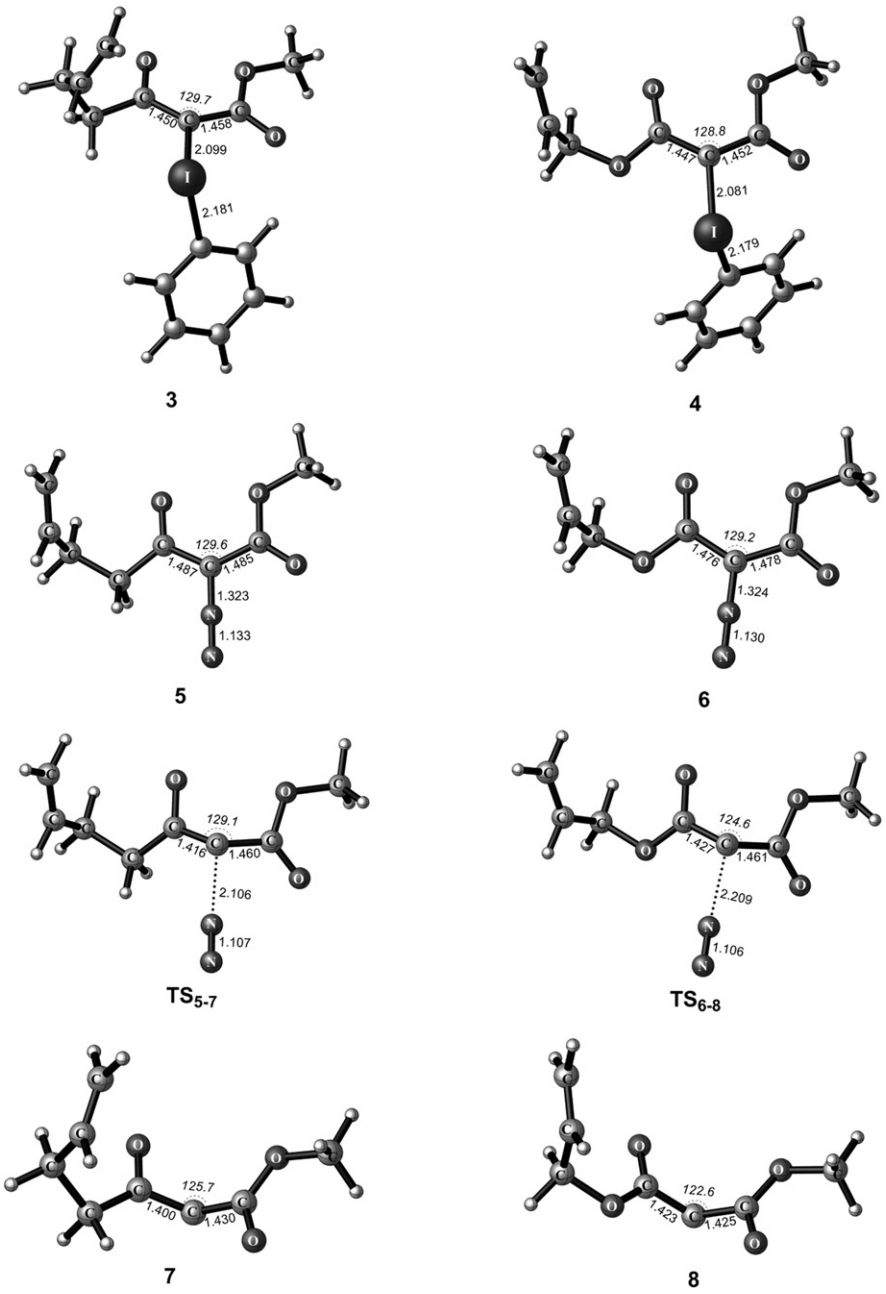

Fig. 2. Equilibrium geometries for the phenyliodonium compounds **3** and **4**, the diazo compounds **5**, **6**, the transition states $\mathbf{TS_{5-7}}$ and $\mathbf{TS_{6-8}}$, and the ketoesteric, **7** and diesteric, **8** carbene molecules computed at the B3LYP/6−31G(d)∪dgdzvp(I) level of theory.

Table 1
Selected electronic parameters of the phenyliodonium ylides **3** and **4**, the diazo compounds **5** and **6**, and the ketoesteric, **7** and diesteric, **8** carbene molecules computed at the B3LYP/6−31G(d)∪dgdzvp(I) level of theory.

Molecule	η	ω[a]	*nec*(X)[b] ns/np	*nec*(C−carbene)[b] 2*s*/2*p*	*bop*[c] C−X	*bop* X−$C_{carbene}$	q_X[d]	$q_{C-carbene}$
3	3.96	1.68	1.77/4.28	1.05/3.50	0.230	0.286	0.91 (0.33)[e]	−0.57 (−0.34)
4	4.02	1.68	1.77/4.26	1.04/3.56	0.237	0.315	0.94 (0.37)	−0.62 (−0.37)
5	4.54	2.29	1.12/3.75	0.91/3.26		0.283	0.09 (0.11)	−0.18 (0.01)
6	4.86	2.15	1.11/3.74	0.90/3.29		0.271	0.11 (0.14)	−0.21 (−0.01)
7	3.98	2.75		1.18/2.72				0.08 (−0.03)
8	3.81	3.11		1.23/2.69				0.05 (−0.02)

[a] Electrophilicity index $\omega = \mu^2/2\eta$, where μ and η are the chemical potential and hardness respectively given approximately by the expressions $\mu = (\varepsilon_{LUMO} + \varepsilon_{HOMO})/2$ and $\eta = (\varepsilon_{LUMO} - \varepsilon_{HOMO})$. η and ω are given in eV.
[b] Natural electron configuration (*nec*).
[c] Bond overlap population (*bop*).
[d] Natural atomic charges; X = I or N.
[e] Figures in parentheses are the Mulliken net atomic charges.

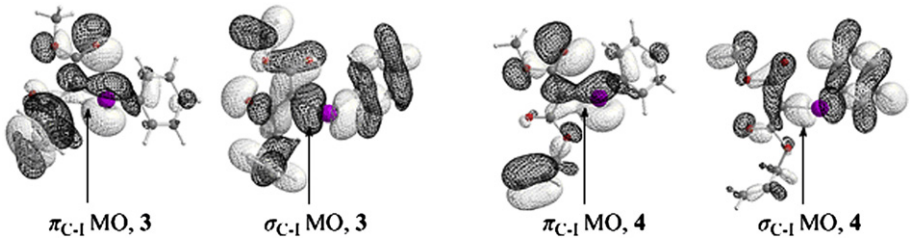

Scheme 5. σ_{C-I}- and π_{C-I}-type MOs of ketoesteric and diesteric iodonium ylides **3** and **4**.

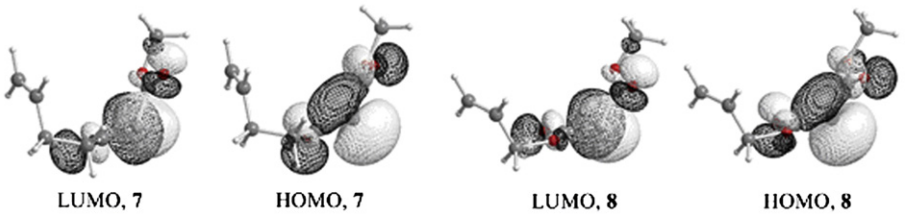

Scheme 6. Frontier molecular orbitals of ketoesteric **7** and diesteric carbene **8**.

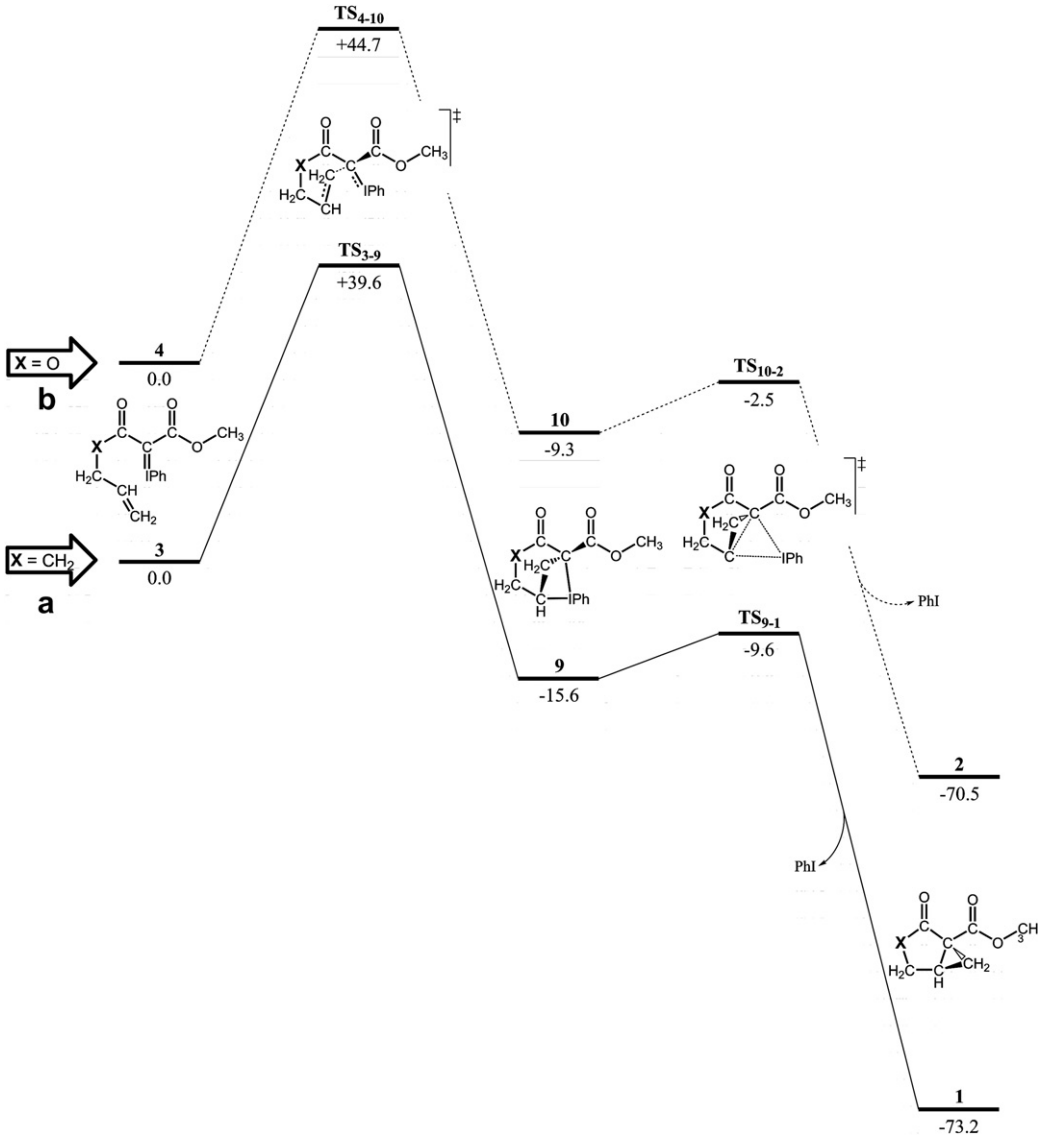

Fig. 3. Energetic ($\Delta_R G^{solv}$, in kcal/mol) reaction profiles for the PhI-assisted intramolecular cyclopropanation of ketoesteric (a) and diesteric (b) phenyliodonium ylides computed at the B3LYP/6−31G(d)∪dgdzvp(I) level of theory.

bond is much stronger than the Ph–I one (Table 1). There are weak σ- and π-type bonding interactions in **3** and **4** located in the C-I bond region described by the HOMO-13 and HOMO-2, respectively (Scheme 5).

The charge distribution on the iodine and the carbene carbon atoms of iodonium ylides **3** and **4** reveals that the C=I bond involves an ionic component as well. Noteworthy is the very low negative Mulliken net atomic charge of −0.03 and −0.02 |e| on the carbene carbon atom in the "free" carbene molecules **7** and **8**, respectively. It should be noted that the natural atomic charges on the carbene C atom are positive amounted to 0.08 and 0.07 |e| for **7** and **8**, respectively, indicating that the carbene carbon atom constitutes an electrophilic center. Carbenes **7** and **8** are easily transformed to the final products **1** and **2**, respectively via transition states $\mathbf{TS_{7\text{-}1}}$ and $\mathbf{TS_{8\text{-}2}}$, with very low activation barriers of 1.7 and 3.9 kcal/mol respectively. Moreover, the uncatalyzed cyclopropanation of the ketoesteric, **3** and the diesteric, **4** iodonium ylides are strongly exergonic, the estimated exergonicities are −73.2 and −70.5 kcal/mol respectively. It is evident that the intramolecular cyclopropanation of ketoesteric phenyliodonium ylides is thermodynamically and kinetically more favored than the cyclopropanation of diesteric phenyliodonium ylides (Fig. 1) in line with experiments. The normal coordinate vectors (arrows) of the vibrational modes corresponding to the imaginary frequency of $\mathbf{TS_{7\text{-}1}}$ and $\mathbf{TS_{8\text{-}2}}$ at 56*i* and 118*i* respectively are those consistent with the intramolecular transformation. The low values of the imaginary frequencies are also compatible with the computed low activation barriers.

Perusal of the frontier molecular orbitals of carbenes **7** and **8** (Scheme 6) reveals that the uncatalyzed intramolecular cyclopropanation reactions of iodonium ylides are driven by the intramolecular HOMO–LUMO interactions in the carbene molecules, since their HOMOs (donor MOs) are π-MOs localized on the ethenyl double bond, while the LUMOs (acceptor MOs) are mainly localized on the electrophilic carbene carbon atom. In other words, the C=C double bond is electrophilicaly attacked by the electrophilic carbene carbon atom, thus forming the cyclopropane ring.

The rate-limiting step in the uncatalyzed cyclopropanation of iodonium ylides corresponds to their dissociation process leading to the formation of the "free" carbene molecules upon reductive elimination of PhI. Thus, the higher dissociation energy of the diesteric iodonium ylide compared to that of the ketoesteric one accounts for the inefficient intramolecular cyclopropanation of the diesteric iodonium ylides observed experimentally. Actually, under mild conditions (P = 1 atm, T = 273 K) the cyclopropanation proceeds easily and in high yields only in the case of the ketoesteric iodonium ylide, while cyclopropanation of the diesteric derivatives proceeds with difficulty and with very low yields (3%) [20,21].

3.2. Uncatalyzed PhI-assisted cyclopropanation mechanism

Next, we considered an alternative possible reaction pathway, in which the phenyliodide fragment remains connected throughout the reaction with the carbene carbon. This alternative reaction path corresponds to a stepwise mechanism, in contrast to the free radical reaction path, which is concerted. The calculated energetic reaction profiles for the alternative uncatalyzed intramolecular cyclopropanation of ketoesteric, **3** and diesteric, **4** iodonium ylides are depicted schematically in Fig. 3.

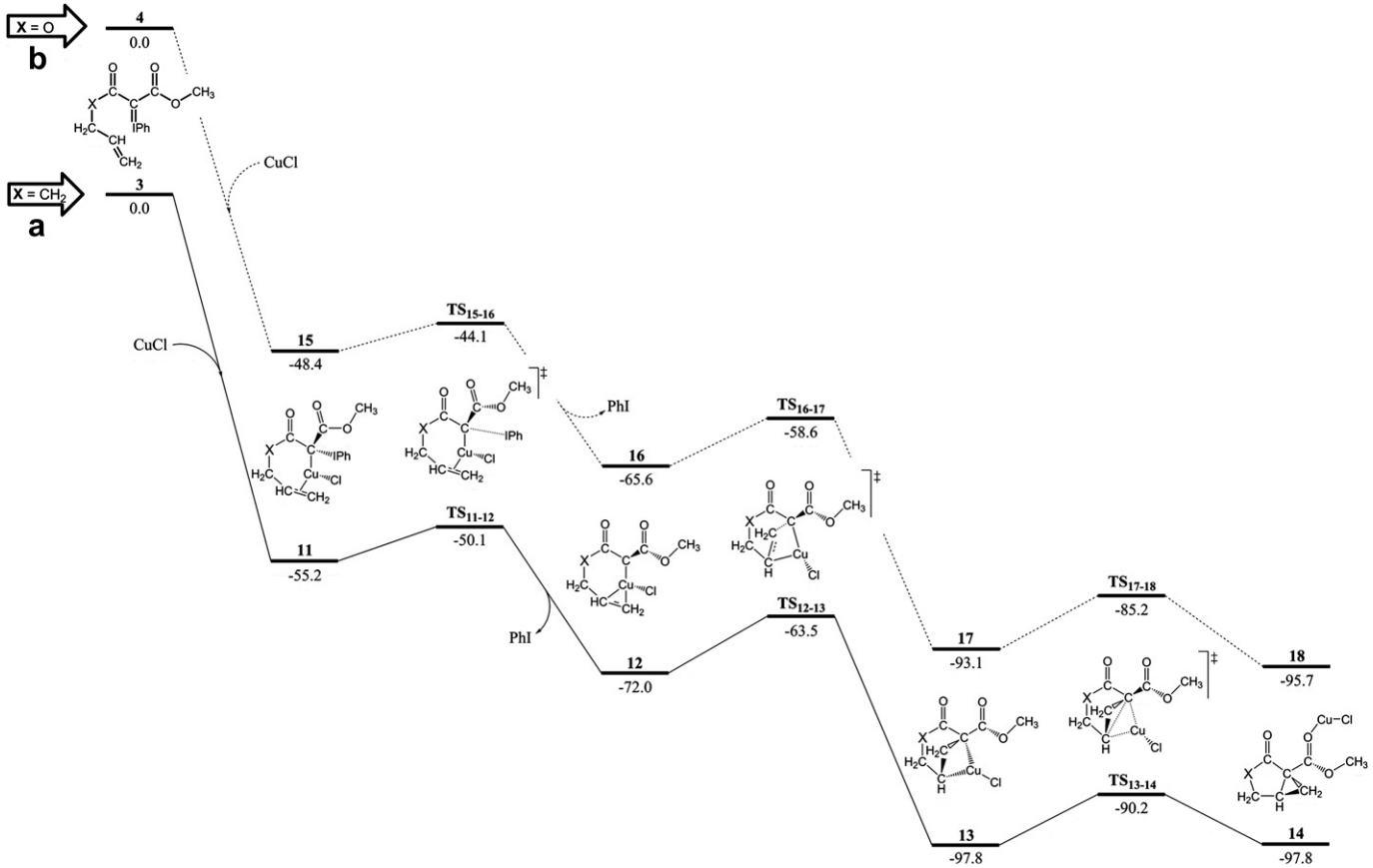

Fig. 4. Energetic ($\Delta_R G^{solv}$, in kcal/mol) reaction profiles for the Cu(I)-catalyzed intramolecular cyclopropanation of ketoesteric (a) and diesteric (b) phenyliodonium ylides computed at the B3LYP/6–31G(d)∪dgdzvp(I) level of theory.

It can be seen that, an intramolecular closure of the ring occurs in the ketoesteric **3** and diesteric **4** compounds, in the presence (coexistence) of PhI forming a six-membered ring (3–9 and 4–10). The activation barriers of the cyclization steps are extremely high being 39.6 and 44.7 kcal/mol respectively. The C–C coupling takes place between the terminal carbon of the olefinic bond and the carbene carbon, which is in contrast with the first mechanism. More specifically, in the transition state the position of the olefinic double bond is out of plane and vertical to the I–$C_{carbene}$ bond, in order to achieve the closure of the ring. The cyclization step for the ketoesteric and diesteric phenyliodonium ylides is exergonic by −15.6 and −9.3 kcal/mol respectively. In the resulting structures **9** and **10** the phenyliodide is attached to the two carbons of the ring and might be responsible for the formation of the cyclopropane ring (9 to 1 and 10 to 2). Finally, the transition states which connect the final products with the intermediates **9** and **10**, surmount a small activation barrier of only 6.0 and 6.9 kcal/mol respectively, while the formation of the final product is energetically highly favorable ($\Delta G = -57.6$ and −61.2 kcal/mol respectively). Overall, the alternative reaction path was found to be energetically unfavorable relative to the concerted reaction path.

3.3. Cu(I)-catalyzed cyclopropanation mechanism

Let us now go deeper into the mechanism of the Cu(I)-catalyzed (using CuCl as catalyst) intramolecular cyclopropanation of the ketoesteric and diesteric iodonium ylides **3** and **4** unraveling the role played by the catalyst. The energy profiles of the catalyzed reactions are depicted schematically in Fig. 4.

The equilibrium structures of the relevant stationary points in the PES of the Cu(I)-catalyzed cyclopropanation of phenyliodonium ylides **3** and **4**, computed at the B3LYP/6–31G(d)∪dgdzvp(I) level of theory are shown in Figs. 5 and 6, respectively.

Attachment of the iodonium ylide to the CuCl catalyst leads to the lengthening of the I–$C_{carbene}$ bonds with respect to **3** and **4** by 0.12 and 0.14 Å respectively. It should be noticed that the coordination of the olefinic bond to the copper center results in the lengthening of the C=C double bond about 0.06 Å for both cases. In accordance, the ketoesteric or diesteric carbene C adopt a pseudo-T-shaped structure. The formation of intermediates **11** and **15** is predicted to be highly exergonic by −55.2 and −48.4 kcal/mol respectively at the B3LYP level of theory. The intermediates **11** and

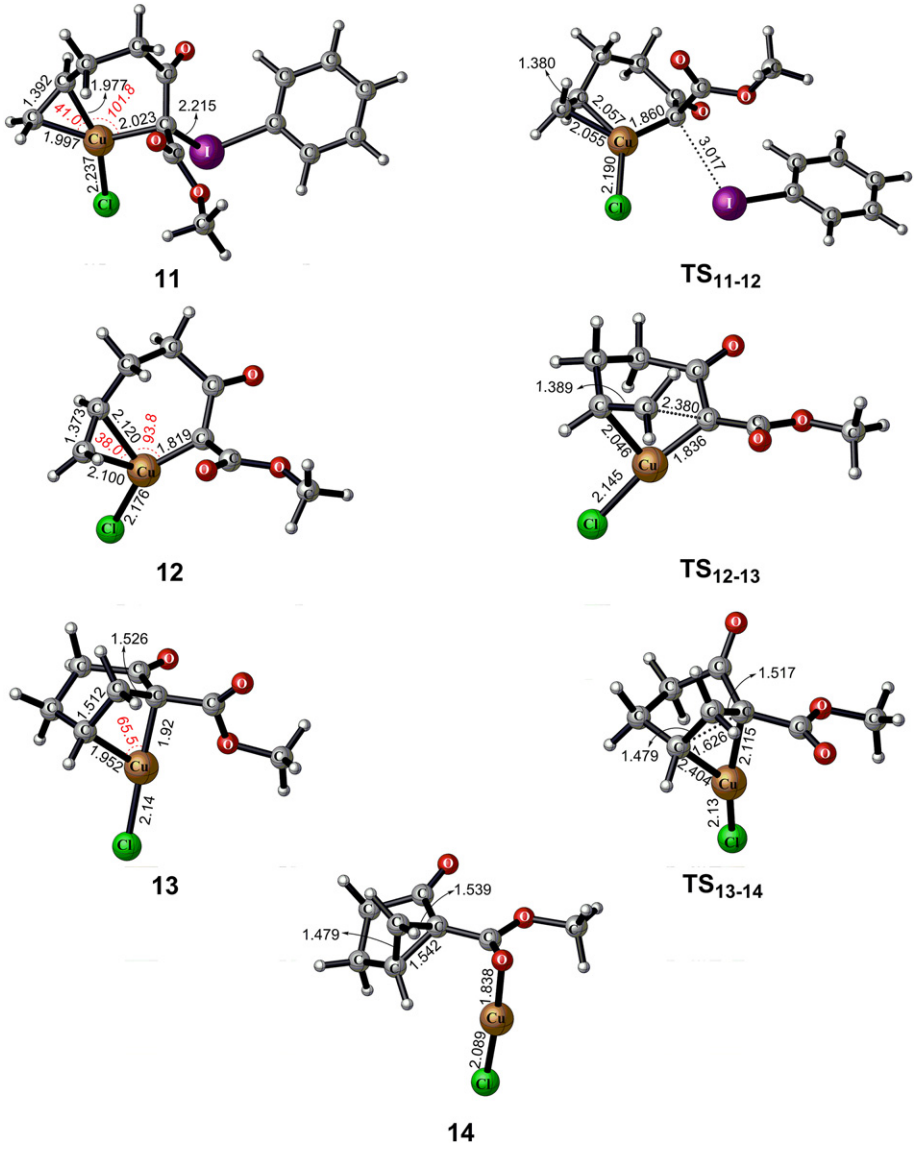

Fig. 5. Equilibrium geometries of the relevant stationary points in the PES of the Cu(I)-catalyzed cyclopropanation of the ketoesteric phenyliodonium ylide **3**.

15 are subsequently transformed to intermediates **12** and **16** via transition states $\mathbf{TS_{11-12}}$ ($\nu = 51i$) and $\mathbf{TS_{15-16}}$ ($\nu = 52i$) with low activation barriers of 5.1 and 4.3 kcal/mol respectively, after the dissociation of the iodobenzene. This step corresponds to an exergonic process with exergonicities of 16.8 and 17.2 kcal/mol respectively.

The next step of the reaction path involves the formation of the six-membered ring through transition states $\mathbf{TS_{12-13}}$ ($\nu = 137i$) and $\mathbf{TS_{16-17}}$ ($\nu = 201i$), yielding intermediates **13** and **17** with relative low activation barriers of 8.5 and 7.0 kcal/mol in terms of ΔG^{solv} respectively. The lower activation barrier of this step illustrates the more facile cyclization that occurs in the presence of the catalyst as compared to the PhI-assisted mechanism. The transition states $\mathbf{TS_{12-13}}$ and $\mathbf{TS_{16-17}}$ exhibit some identical structural features in comparison with the $\mathbf{TS_{3-9}}$ and $\mathbf{TS_{4-10}}$ respectively. Insomuch that, the shape of geometries in the transition states are very close, and in particular, the distance of the C–C bond which is going to be created in $\mathbf{TS_{12-13}}$, is only 0.26 Å longer than that in $\mathbf{TS_{3-9}}$, while the olefinic double bond distance is almost the same in the two TS's. Also, the bond distances of the distant carbons in the pre-

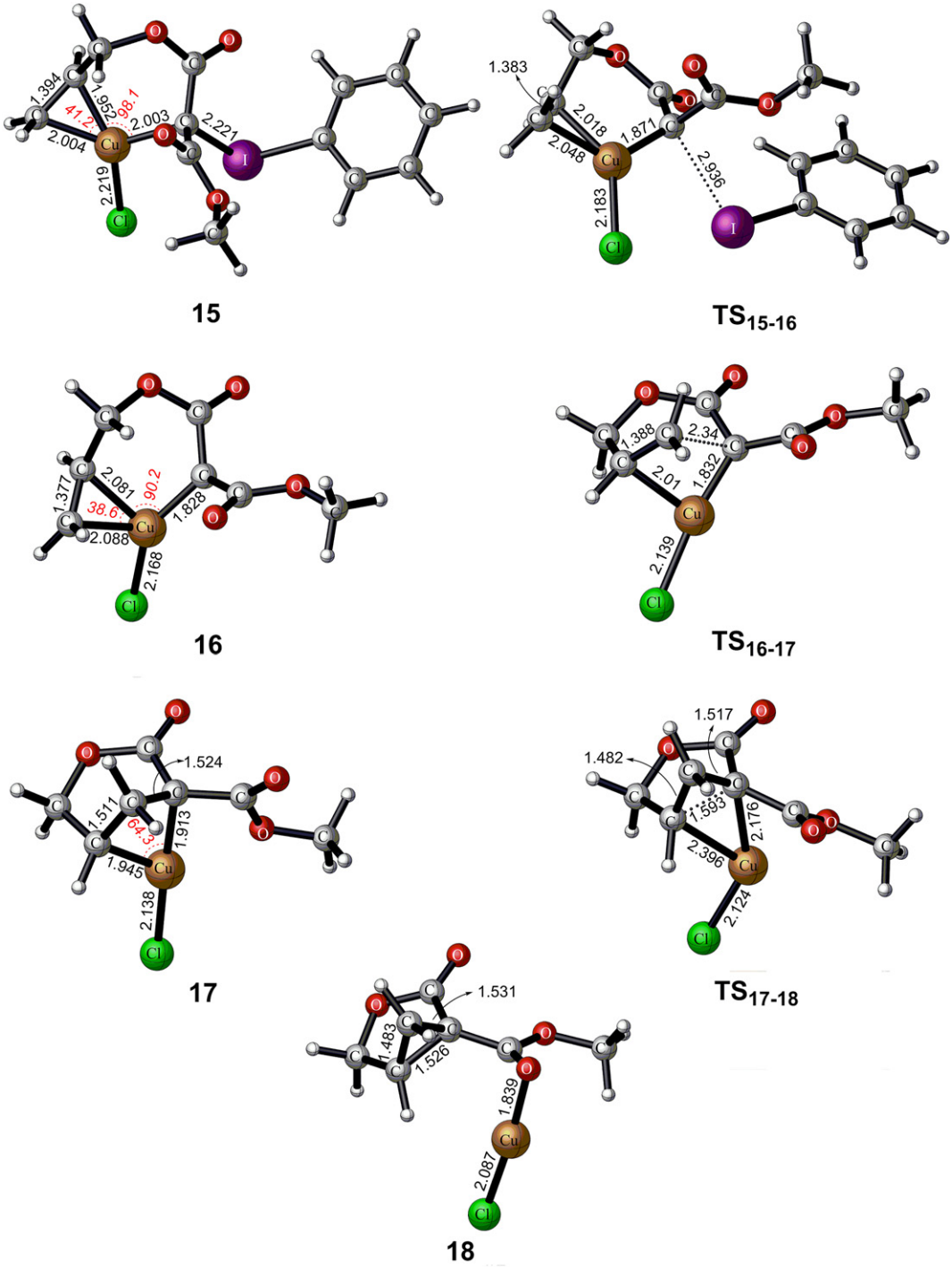

Fig. 6. Equilibrium geometries of the relevant stationary points in the PES of the Cu(I)-catalyzed cyclopropanation of the diesteric phenyliodonium ylide **4**.

cyclopropanic ring differ by only 0.13 Å in the aforementioned transition states. Finally, the angle that is formed by the three carbons involved in the formation of the cyclopropanic ring is only 6 degrees bigger in **TS$_{3-9}$** than in **TS$_{12-13}$**, being 100 and 94^0 respectively. The same trends have also been observed for the diesteric analogue. In the vibrational modes corresponding to the imaginary frequencies of **TS$_{12-13}$** and **TS$_{16-17}$**, the dominant motions involve the stretching of the terminal carbon of the olefinic double bond towards the $C_{carbene}$ atom. These transition states could be characterized as late transition states, as it can be seen by the geometric features of the corresponding structures (Figs. 5 and 6).

The intermediates **13** and **17** are found to be more stable than intermediates **12** and **16** by 25.8 and 27.5 kcal/mol respectively (in terms of $\Delta_R G^{solv}$). During the course of the C–C coupling process the two carbons interact to form the cyclopropanic ring via transition states **TS$_{13-14}$** and **TS$_{17-18}$**, surmounting a relatively low energy barrier of 7.4 and 7.9 kcal/mol, respectively. Regarding the C–C bond distances of the remaining bonds of the cyclopropanic ring in both ketoesteric and diesteric species, it was found to be almost equal to the respective C–C bond lengths of the corresponding products. This means that **TS$_{13-14}$** and **TS$_{17-18}$** are late transition states. In the vibrational modes corresponding to the imaginary frequencies of **TS$_{13-14}$** ($\nu = 99i$) and **TS$_{17-18}$** ($\nu = 94i$), the dominant motions involve the C–C coupling and the concomitant removal of CuCl catalyst. Finally, detachment of the catalyst from **14** and **18** affords the cyclopropanation products **1** and **2** respectively. The estimated coordination energies of **1** and **2** to CuCl amount to −24.6 and −25.2 kcal/mol respectively and are about two times smaller compared to the binding energies of **3** and **4** (−55.2 and −48.4 kcal/mol) respectively. Therefore, the regeneration of the CuCl catalyst will occur easily after the dissociation of the products **1** and **2** upon coordination of **3** and **4** respectively.

In summary the rate-limiting step for cyclopropanation of ketoesteric iodonium ylides catalyzed by CuCl is predicted to be the step of formation of the six-membered ring, while for the diesteric one it is predicted to be the formation of the cyclopropanic ring. This is in contrast with the PhI-assisted mechanism, where the dissociation step of the phenyliodide was the rate-limiting step. It should be noted that in almost all Cu(I) complexes (except the last intermediate) involved along the two possible reaction pathways the copper central atom is three-coordinated adopting a planar T-shaped structure. On the other hand, all attempts that were made to support the mechanism proposed by Moriarty and co-workers [26–29] in which the iodobenzene is attached on the carbene C in the presence of catalyst were unsuccessful.

4. Conclusions

In summary, this report substantiates the CuCl-assisted cyclopropanation of iodonium ylides only for the diesteric derivatives **2** and the diazo analogues **5** and **6** via stabilization of the respective carbene upon complexation with the metal center. For the ketoesteric iodonium ylides **1** the CuCl catalyst does not affect the kinetics of the intramolecular cyclopropanation reactions which could proceed easily without the catalyst. This is consistent with the available experimental observations that cyclopropanation of ketoesteric iodonium ylides proceeds easily both in the absence and in the presence of catalytic amounts of CuCl affording the same products with identical stereoisomer ratio. In contrast, the cyclopropanation of diesteric iodonium ylides proceeds only in the presence of CuCl catalyst.

Appendix A. Supplementary material

The Cartesian coordinates and energies of all stationary points are compiled in Table S1. Supplementary data associated with this article can be found, in the online version, at doi:10.1016/j.jorganchem.2010.05.013.

References

[1] M.P. Doyle, Acc. Chem. Res. 19 (1986) 348.
[2] M.P. Doyle, M.A. McKervey, T. Ye, Modern Catalytic Methods for Organic Synthesis with Diazo Compounds. John Wiley & Sons, New York, Inc, 1998.
[3] T. Ye, M.A. McKervey, Chem. Rev. 94 (1994) 1091.
[4] M.P. Doyle, M.N. Protopopova, Tetrahedron 54 (1998) 7919.
[5] H. Brunner, Angew. Chem. Int. Ed. Engl. 31 (1992) 1183.
[6] A. Padwa, K.E. Krumpe, Tetrahedron 48 (1992) 5385.
[7] V.K.D.A. Singh, G. Sekar, Synthesis (1997) 137.
[8] T. Rasmussen, J.F. Jensen, N. Ostergaard, D. Tanner, T. Ziegler, P.-O. Norrby, Chem. Eur. J. (2002) 177.
[9] V.V. Zhdankin, P.J. Stang, Chem. Rev. 102 (2002) 2523.
[10] P.J. Stang, J. Org. Chem. 68 (2003) 2997.
[11] W. Kirmse, Angew. Chem. Int. Ed. 42 (2003) 1088.
[12] H. Lebel, J.-F. Marcoux, C. Molonaro, A.B. Charette, Chem. Rev. 103 (2003) 977.
[13] T. Katsuki, Compr. Coord. Chem. II 9 (2004) 207.
[14] T. Sawada, M. Nakada, Adv. Synth. Catal. 347 (2005) 1527.
[15] R.M. Moriarty, J. Org. Chem. 70 (2005) 2893.
[16] J.K. Gallos, T.V. Koftis, A.E. Koumbis, J. Chem. Soc., Perkin Trans. 1 (1994) 611 and references therein.
[17] A. Varvoglis, The Organic Chemistry of Polycoordinated Iodine. VCH Publishers, Weinheim, 1992.
[18] A. Varvoglis, Hypervalent Iodine in Organic Synthesis. Academic Press, San Diego, 1997.
[19] G. Maas, Chem. Soc. Rev. 33 (2004) 183.
[20] J.K. Gallos, T.V. Koftis, Z.S. Massen, C.C. Dellios, I.T. Mourtzinos, E. Coutouli-Argyropoulou, A.E. Koumbis, Tetrahedron 58 (2002) 8043.
[21] J.K. Gallos, Z.S. Massen, T.V. Koftis, C.C. Dellios, Tetrahedron Lett. 42 (2001) 7489.
[22] P. Müller, D. Fernandez, Helv. Chim. Acta 78 (1995) 947.
[23] P. Müller, C. Bolea, Synlett (2000) 826.
[24] P. Müller, C. Bolea, Helv. Chim. Acta 84 (2001) 1093.
[25] P. Müller, Acc. Chem. Res. 37 (2004) 243.
[26] R.M. Moriarty, O. Prakash, R.K. Vaid, L. Zhao, J. Am. Chem. Soc. 111 (1989) 6443.
[27] R.M. Moriarty, O. Prakash, R.K. Vaid, L. Zhao, J. Am. Chem. Soc. 112 (1990) 1297.
[28] R.M. Moriarty, J. Kim, L. Guo, Tetrahedron Lett. 34 (1993) 4129.
[29] R.M. Moriarty, E.J. May, L. Guo, O. Prakash, Tetrahedron Lett. 39 (1998) 765.
[30] M.B. Camacho, A.E. Clark, T.A. Liebrecht, J.P. DeLuca, J. Am. Chem. Soc. 122 (2000) 5210.
[31] M.J. Frisch, G.W. Trucks, H.B. Schlegel, G.E. Scuseria, M.A. Robb, J.R. Cheeseman, J.A. Montgomery Jr., T. Vreven, K.N. Kudin, J.C. Burant, J.M. Millam, S.S. Iyengar, J. Tomasi, V. Barone, B. Mennucci, M. Cossi, G. Scalmani, N. Rega, G.A. Petersson, H. Nakatsuji, M. Hada, M. Ehara, K. Toyota, R. Fukuda, J. Hasegawa, M. Ishida, T. Nakajima, Y. Honda, O. Kitao, H. Nakai, M. Klene, X. Li, J.E. Knox, H. P. Hratchian, J.B. Cross, V. Bakken, C. Adamo, J. Jaramillo, R. Gomperts, R. E. Stratmann, O. Yazyev, A.J. Austin, R. Cammi, C. Pomelli, J.W. Ochterski, P. Y. Ayala, K. Morokuma, G.A. Voth, P. Salvador, J.J. Dannenberg, V.G. Zakrzewski, S. Dapprich, A.D. Daniels, M.C. Strain, O. Farkas, D.K. Malick, A.D. Rabuck, K. Raghavachari, J.B. Foresman, J.V. Ortiz, Q. Cui, A.G. Baboul, S. Clifford, J. Cioslowski, B.B. Stefanov, G. Liu, A. Liashenko, P. Piskorz, I. Komaromi, R. L. Martin, D.J. Fox, T. Keith, M.A. Al-Laham, C.Y. Peng, A. Nanayakkara, M. Challacombe, P.M.W. Gill, B. Johnson, W. Chen, M.W. Wong, C. Gonzalez, J. A. Pople, Gaussian 03, Revision E.01. Gaussian, Inc, Wallingford, CT, 2004.
[32] A.D. Becke, J. Chem. Phys. 96 (1992) 2155.
[33] A.D. Becke, J. Chem. Phys. 98 (1993) 5648.
[34] C. Lee, W. Yang, R.G. Parr, Phys. Rev. B 37 (1988) 785.
[35] P.J. Stephens, F.J. Devlin, C.F. Chabalowski, M.J. Frisch, J. Phys. Chem. 98 (1994) 11623.
[36] P.J. Stephens, F.J. Devlin, C.S. Ashvar, K.L. Bak, P.R. Taylor, M.J. Frisch, ACS Symp. Ser. 629 (1996) 105.
[37] M. Diedenhofen, T. Wagener, G. Frenking, T. Cundari, Computational Organometallic Chemistry. Marcel Dekker, New York, 2001.
[38] S.H. Vosko, L. Wilk, M. Nusair, Can. J. Phys. 58 (1980) 1200.
[39] J. Baker, M. Muir, J. Andzelm, A. Scheiner, in: B.B. Laird, R.B. Ross, T. Ziegler (Eds.), Chemical Applications of Density-Functional Theory, ACS Symposium Series 629, American Chemical Society, Washington, DC, 1996.
[40] L.A. Curtiss, K. Raghavachari, P.C. Redfern, J.A. Pople, J. Chem. Phys. 106 (1997) 1063.
[41] M. Böhme, G. Frenking, Chem. Phys. Lett. 224 (1994) 195.
[42] M.P. Head-Gordon, M.J. Frisch, Chem. Phys. Lett. 153 (1988) 503.
[43] C. Gonzalez, H.B. Schlegel, J. Chem. Phys. 90 (1989) 2154.
[44] C. Gonzalez, H.B. Schlegel, J. Phys. Chem. 94 (1990) 5523.
[45] J. Tomasi, B. Mennucci, R. Cammi, Chem. Rev. 105 (2005) 2999.